J. Astrophys. Astr. (1986) **7,** 17–28

Towards a Physical Model for Galactic Rotation Curves

Ramanath Cowsik & Pranab Ghosh *Tata Institute of Fundamental Research, Homi Bhabha Road, Colaba, Bombay 400005*

Received 1985 April 4; accepted 1985 October 4

Abstract. Extensive and meticulous observations of the rotation curves of galaxies show that they are either flat or gently going up, but rarely decreasing, at large galactocentric distances. Here we show that the gravitational potential which would lead to such rotation curves arises naturally when the visible matter modelled as a collisionless Maxwellian gas is embedded in a dark halo of collisionless particles with a much higher dispersion in velocities.

Key words: galaxies, rotation curve—galaxies, dark matter—neutrino, mass

1. Introduction

Important insights into the structure and dynamics of galaxies have come from systematic and extensive observations of their rotation curves (Rubin 1979; Rubin, Ford & Thonnard 1980, 1982; Bosma 1978 and references therein). Even though the rotation curves in the central regions show great diversity and individuality in different galaxies, they exhibit a remarkable universality at larger galactocentric distances. Almost all the curves observed so far are either sensibly flat or faintly rising up to the largest observed distances. Indeed Rubin (1979) remarks ' . . . it is almost impossible to identify a galaxy with a falling optical rotation curve . . . nearly constant velocities and significant mass at large r are the rule . . . '. For the bright spirals the velocities increase rapidly with the radial distance from the centre, go through a maximum, fall initially and slowly increase to values ~ 150–300 km s^{-1} at large distances. Over this general pattern, velocity undulations of amplitude $\lesssim$ 20 km s^{-1} are seen coincident with the positions of spiral arms.

These features are usually understood in terms of a three-component empirical model, the components being a disc, a nuclear bulge and a halo or corona. The density distributions of these components are adjusted to reproduce the observed rotation curve (Einasto 1970; Ostriker & Caldwell 1979; Bahcall, Schmidt & Soneira 1982), which is obtained from the condition that the centrifugal force in a circular orbit equals the galactocentric force derived from the total potential Ψ due to these distributions, *i.e.*,

$$V_r^2 = -r\frac{\partial \Psi}{\partial r}. \tag{1}$$

Here V_r. is the (circular) rotation velocity and r is the galactocentric distance. At large distances, the observations cited above demand that $\partial\Psi/\partial r \sim r^{-\alpha}$, with $\alpha \lesssim 1$. By

analyzing a sample of 21 Sc galaxies (Burstein *et al.* 1982) and 23 Sb galaxies (Rubin, Ford & Thonnard 1982), Rubin and her co-workers have shown that α = 0.7–0.8, so that $V_r \sim r^{0.1-0.15}$.

The purpose of this paper is to show that such a potential arises naturally when the visible matter in the galaxy is embedded in a dark halo of collisionless gas whose velocity dispersion and spatial extent are much larger than those of the visible matter. In Section 2, we model the visible matter consisting predominantly of stars as a Maxwellian gas and calculate its self-consistent density profile; the rotation curves and the profiles of luminosity thus calculated reproduce the observations remarkably well. In Section 3 we investigate the nature of the constituents of the extended cloud of dark matter and comment on the suitability of neutrinos as the dark matter (Cowsik & McClelland 1973).

2. The model

We model the visible matter in the galaxies as a Maxwellian gas embedded in an extended cloud of collisionless particles with a much larger dispersion in their velocities. Binney (1982a, b) has shown that a Maxwellian distribution describes the luminosity profiles of elliptical galaxies well. The same is true for spiral galaxies, as we show below (see Section 2.3). A basic reason for the ubiquity of such a distribution is discussed in Cowsik (1984).

The equilibrium state of such a system is described by the Poisson equation, which, because of linearity, splits into

$$\nabla^2 \Psi_b = 4\pi G \rho_b; \qquad \nabla^2 \Psi_v = 4\pi G \rho_v . \tag{2a; b}$$

Since the dominant constituents of the visible matter are stars, the frequency of collision is very small (Chandrasekhar 1942), the phase-space distribution functions of both the visible and background gases are the solutions of the respective Liouville equations. Qualitatively, the spatial variations in the densities of the two gases will be defined by the characteristic length-scales

$$l_b \sim \left(\frac{k T_b}{4\pi G \rho_b m_b} \right)^{1/2}, \quad \text{and} \quad l_v \sim \left(\frac{k T_v}{4\pi G \rho_v m_v} \right)^{1/2}, \tag{3}$$

and we assume that $l_b \gg l_v$ so that in discussing the spatial variations in ρ_v the background density ρ_b may be treated as constant.

Now, by Jeans' theorem (Jeans 1915; Lynden-Bell 1962), the distribution function for the visible gas can be expressed as any function of $E = \frac{1}{2} m_v v^2 + m_v (\Psi_v + \Psi_b)$, the total energy of a constituent particle. There is evidence that f is Maxwellian (see above):

$$f(v) \sim \exp(-E/kT_v) \sim \exp\left[-\frac{m_v}{kT_v} \left(\frac{1}{2} v^2 + \Psi_v + \Psi_b \right) \right] \tag{4}$$

and

$$\rho_v = \int f \, d^3 v = \rho_0 \exp\left[-\frac{m_v}{kT_v} (\Psi_v + \Psi_b) \right]. \tag{5}$$

We substitute Equation (5) in Equation (2b) and make the resulting equation dimensionless with $\phi = m_v \Psi_v / kT_v$, $\phi_b = m_v \Psi_b / kT_v$ and $\xi = r/l_v$. Here $l_v = (kT_v / 4\pi G \rho_0 m_v)^{1/2}$. With ρ_b constant, the potential due to the background gas

which satisfies the boundary conditions $\phi_b(0) = 0$ is

$$\phi_b(\xi) = \frac{1}{6}\frac{\rho_b}{\rho_0}\xi^2. \tag{6}$$

The potential generated by the visible gas is given by

$$\xi^{-2}(d/d\xi)(\xi^2\, d\phi/d\xi) = \exp\left[-\phi - \frac{1}{6}\frac{\rho_b}{\rho_0}\xi^2\right] \tag{7}$$

for a spherically symmetric configuration. It is interesting to note that an identical equation obtains even for the collisional constituents of visible matter (Chandrasekhar 1939; Cowsik 1984).

The solutions of Equation (7) are obtained by a method described by Emden (1907) and Chandrasekhar (1939). The solutions of interest have finite, nonzero densities at the centre; hence the appropriate boundary conditions at $\xi = 0$ are $\phi = 0$ and $d\phi/d\xi = 0$, which identifies the constant ρ_0 in Equation (5) as the central density of visible matter. The numerical computation assumes the starting solution near the origin as the series $\phi = a\xi^2 + b\xi^4 + c\xi^6 + \ldots$ whose coefficients are found to be $a = 1/6$, $b = -(1+\rho_b/\rho_0)/120$, and $c = (1+5\rho_b/\rho_0)(1+5\rho_b/8\rho_0)/1890$. The potential ϕ for larger values ζ of are obtained by standard numerical methods of integration o Equation (7).

The rotation curves derived from this potential are shown in Fig. 1(a), for various values of ρ/ρ_b. The curves are drawn in terms of dimensionless variables

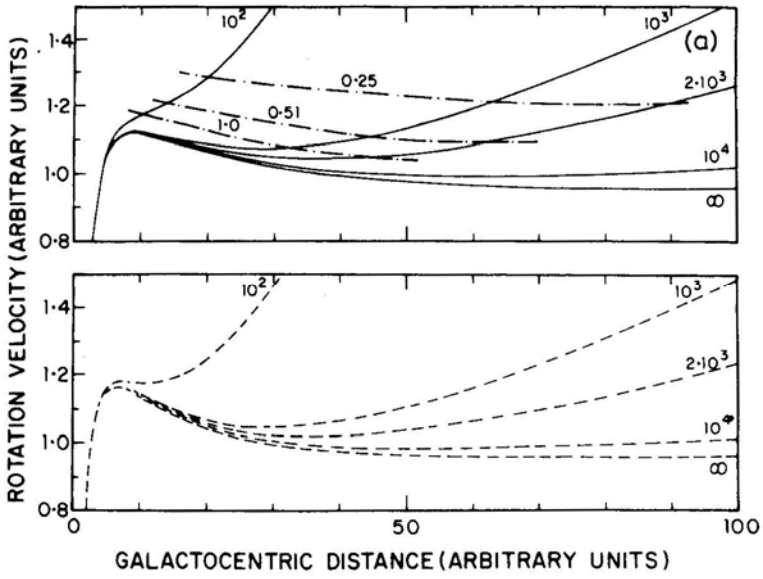

Figure 1(a). Model rotation curves in dimensionless variables (see text). Upper panel: For spherically symmetric distribution of visible gas. Solid lines are rotation curves, each labelled by its value of (ρ/ρ_b). Chain-dotted lines are isodensity contours, each labelled by its value of (ρ_v/ρ_b). The very central parts of the rotation curves are obvious and not shown. Lower panel: for disc distribution of visible gas. Dashed lines are rotation curves, each labelled by its value of (σ/σ_b).

$v = V_r/(2kT_v/m_v)^{1/2}$ and ξ Flat and gently rising rotation curves arise naturally in this model. This can be seen qualitatively by noting that when the background gas is absent the visible matter has an Emden distribution, *i.e.* $\rho_v \sim r^{-2}, \partial\Psi_v/\partial r \sim r^{-1}$ and $r(\partial\psi_v/\partial r)$ constant; *i.e.* an exactly flat rotation curve results. The effect of the background is felt through its contribution to the potential $\psi_b \sim r^2$ which cuts ρ_v off sharply for larger, so that $\partial\psi_v/\partial r$ drops faster than r^{-1}, and the visible matter no longer produces a flat rotation curve by itself. But the sum of the gradients of the two potentials, one falling faster than r^{-1} and the other rising as r^{+1}, yields the requisite gently rising behaviour for the rotation curves. The rotation curves do not rise indefinitely, of course. For $r \gtrsim l_b$, the density of dark matter falls and consequently the rotation curve begins to fall gently. For typical velocity dispersion $v_b \sim 1500$ km s^{-1} and $\rho_b \sim 10^{-25}$ g cm^{-3} (see Section 3) l_b turns out to be ~ 150 kpc.

In order to show that the basic features of the rotation curves are independent of the detailed three-dimensional shape of the visible matter distribution, we have derived rotation curves also for disc distributions which are obtained by allowing the visible matter to collapse on to a plane perpendicular to the rotation axis. The projected surface density $\sigma(\varpi)$ as a function of the radial distance ϖ on the disc is simply

$$\sigma(\varpi) = 2\int_0^\infty \rho_v\left(\sqrt{\varpi^2 + z^2}\right) dz. \tag{8}$$

The potential of such a disc can be expressed in the computationally useful form

$$\Psi_d(\varpi) = -4G\int_0^\infty \sigma(\varpi')\left(\frac{\varpi'}{\varpi_>}\right) K\left(\frac{\varpi_<}{\varpi_>}\right) d\varpi' \tag{9}$$

Here $\varpi_>$ ($\varpi_<$) is the larger (smaller) of ϖ and ϖ', and K is the complete elliptic integral of the first kind. The rotation curves due to the potential of the disc are also shown in Fig. 1(a), (for various values of σ_0/σ_b, where $\sigma_b = 6\rho_b l_v$). It is seen that these are almost identical to those for a spherical distribution of visible matter.

2.1 *Comparison with Observed Rotation Curves*

Optically observed rotation curves of spiral galaxies are usually displayed in terms of radii expressed as fractions of the isophotal radius, R_{25} (= radius where surface brightness is 25 mag arcsec^{-2}). The analogous coordinate in our model is the fraction of the isodensity radius R_{ρ_v} which can be read off from the isodensity contours in Fig. 1(a). Fig. 1(b) shows the model rotation curves in terms of $R_{0.25}$ (radius where $\rho_v/\rho_b = 0.25$), for different values of (ρ_0/ρ_b). Figs 1(c) and (d) show the optical rotation curves for Sb and Sc galaxies respectively, for different luminosities in each class (Rubin, Ford & Thonnard 1980, 1982). Galaxies with higher ρ_0 have higher luminosities: hence we arrange the galaxies by central density in the model curves and by luminosity in the observed ones. No attempt at fitting has been made; the only scaling done was that necessary to obtain the absolute velocity scale for the model rotation curves.

The similarity between theory and observation is clear, and becomes remarkable when individual peculiarities of galaxies are averaged out. as in the 'synthetic' rotation curves given by Rubin (1983), reproduced in Fig. 1(e). The dominant correlation

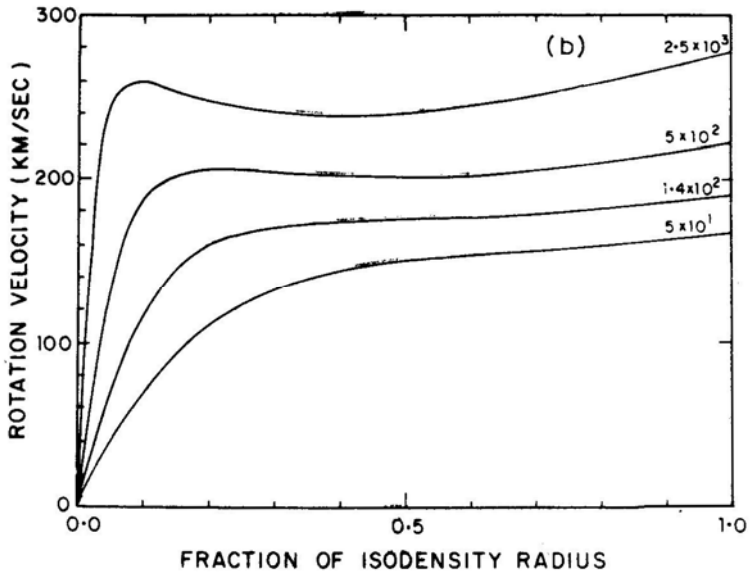

Figure 1(b). Model rotation curves in physical variables, arranged in order of increasing visible matter density. Each curve is labelled by its value of (ρ_0/ρ_b). The isodensity radius used is $R_{0.25}$ where $(\rho_v/\rho_b)= 0.25$.

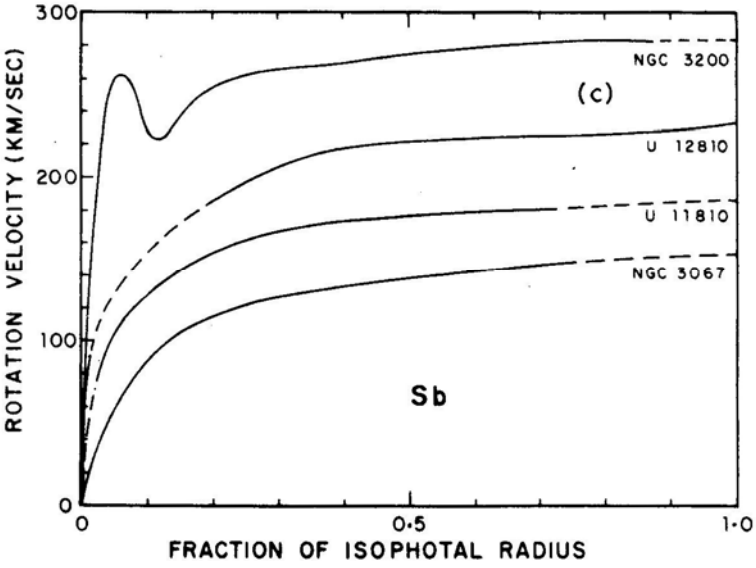

Figure 1(c). Observed rotation curves for Sb galaxies, arranged in order of increasing luminosity (after Rubin, Ford & Thonnard. 1982). The isophotal radius used is R_{25}, where the surface brightness is 25 mag arcsec^{-2}. Data not available in dashed parts of the curves.

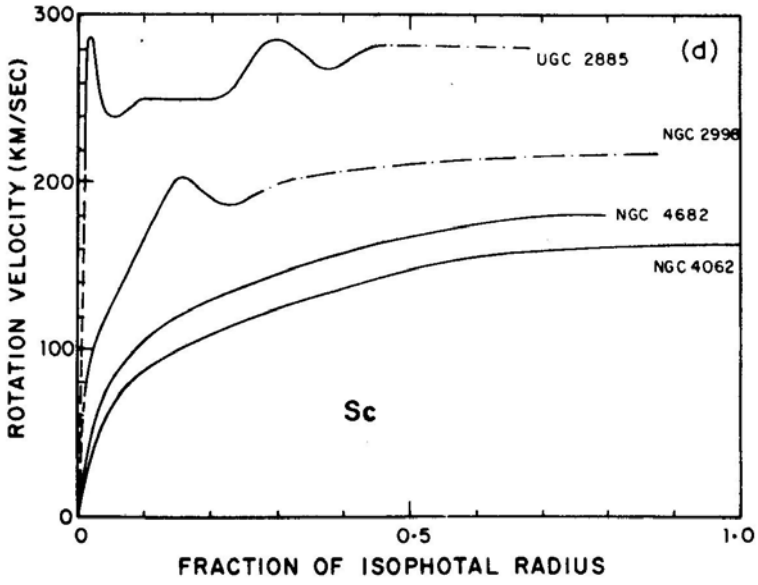

Figure 1(d). Observed rotation curves for Sc galaxies, arranged in the order of increasing luminosity (after Rubin, Ford & Thonnard 1980). Isophotal radius as before. In chain-dotted parts, wiggles containing regions of (unphysical) faster-than-Keplerian fall have been smoothed according to the prescription given by Rubin, Ford & Thonnard (1980).

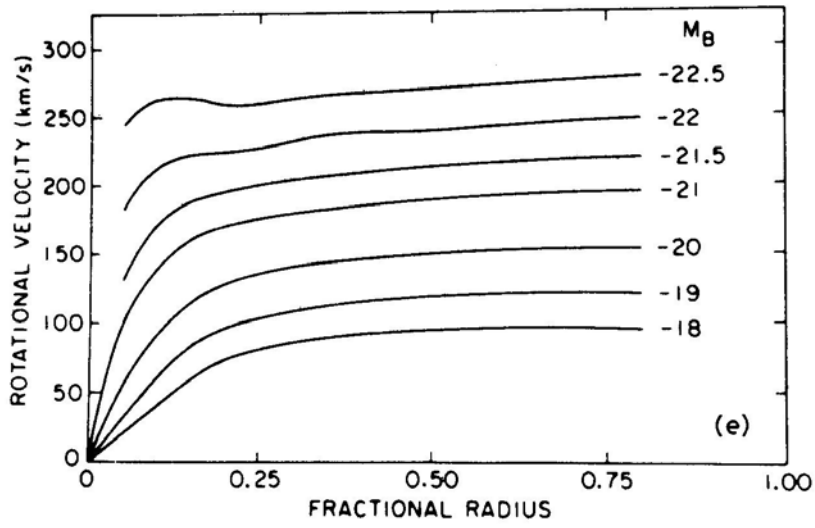

Figure 1(e). 'Synthetic' observed rotation curves for Sb galaxies, arranged in order of increasing luminosity, reproduced from Rubin (1983). The systematic progression in the form of the rotation curve with luminosity is remarkably similar to that in Fig. 1(b).

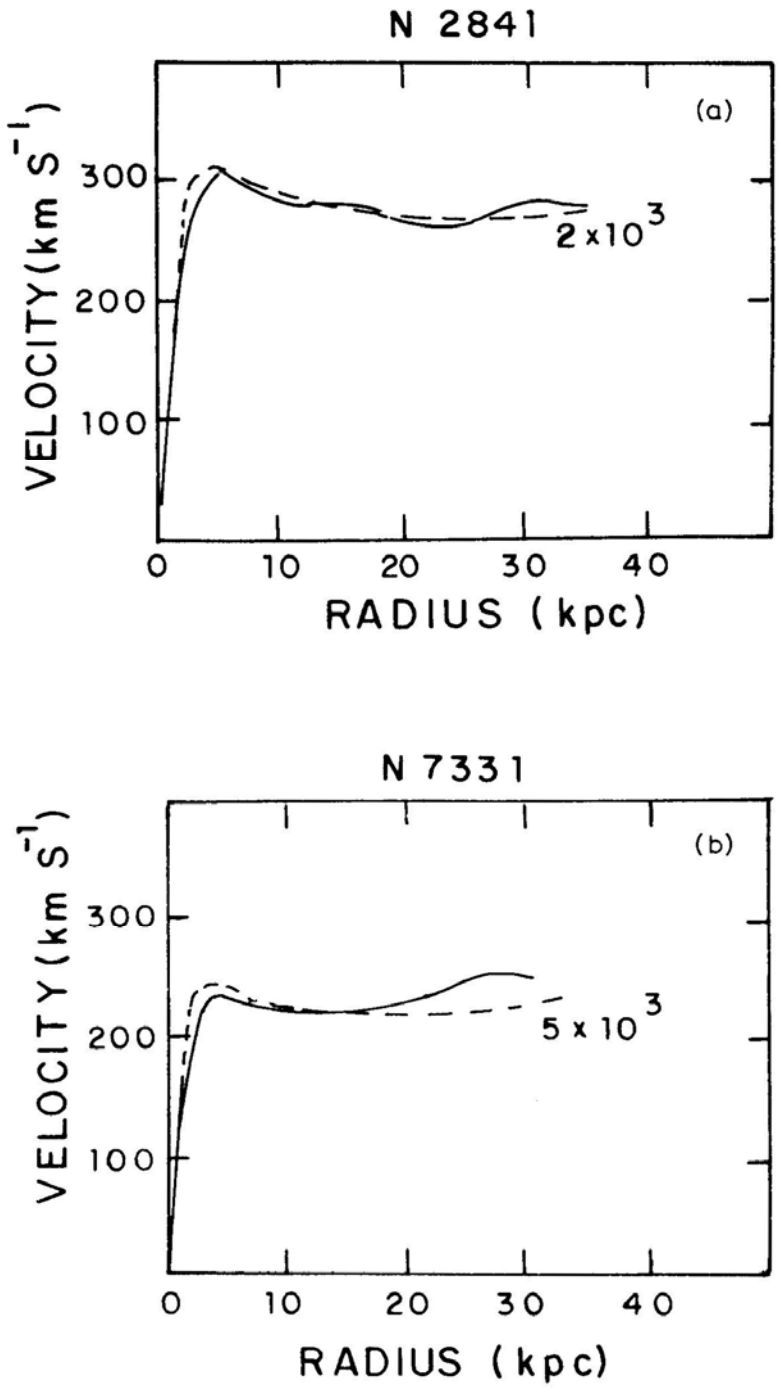

Figure 1(f). HI rotation curves for (a) NGC 2841 and (b) NGC 7331 (from Bosma 1981), compared with model rotation curves. Each model curve is labelled by its value of (ρ_0/ρ_b).

between the luminosity of the galaxy and the form of its rotation curve, so strong as to be proposed as a method of measuring luminosity (Rubin 1983), is almost identical in Figs 1(b) and (e), namely, that with *increasing* ρ_0 and luminosity, rotation velocities rise rapidly at a *smaller* fractional radius, attain *higher* maxima, and have a *longer,* nearly flat portion (Rubin, Ford & Thonnard 1982; Rubin 1983).

Hi rotation curves for spirals are often observed well beyond the optical radius, sometimes upto 2–5 times R_{25} (Bosma 1981; Wevers 1984). Our model curves agree with these observations. Two examples (NGC 2841 and 7331), using Bosma's (1981) observations, are shown in Fig. 1(f). Note that the values of the parameter (ρ_0 / ρ_b) used in these fits are exactly the same as those inferred from fitting the luminosity profiles of these two spirals (see below). This underscores the self-consistency of our model.

A preliminary study of the rotation curves of elliptical galaxies also shows agreement with our model. Detailed results will be presented elsewhere.

2.2 *Luminosity Profiles of Spirals*

A considerable body of data on the luminosity profiles of spiral galaxies has been collected (Kormendy 1977; van der Kruit 1979; Burstein 1979; Boroson 1981; van der Kruit & Searle 1981, 1982). These profiles are usually analyzed in terms of exponential

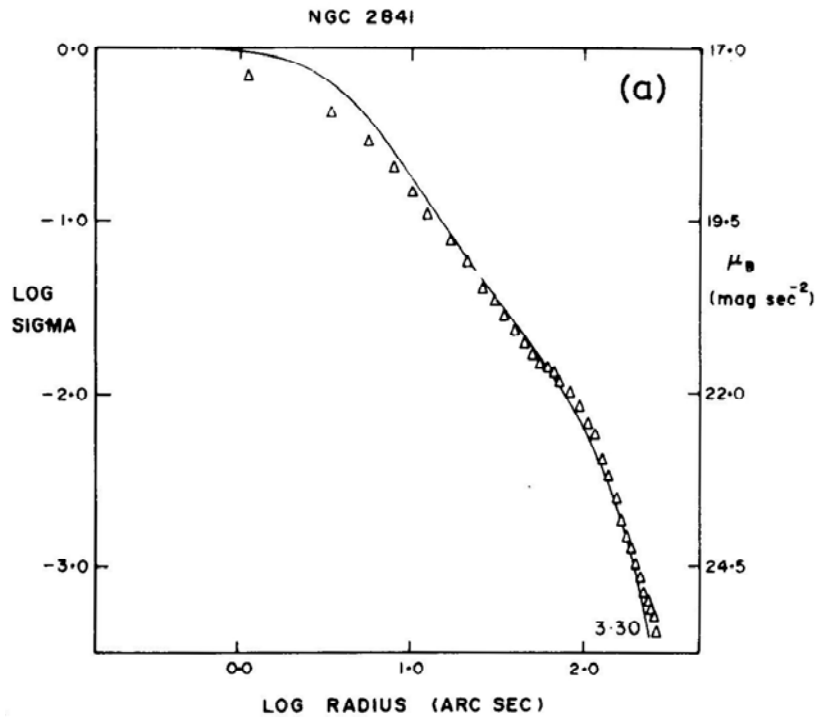

Figure 2. Observed luminosity profiles of spirals compared with model profiles. Triangles are data points for (a) NGC 2841 (from Boroson 1981), (b) NGC 7331 (from Boroson 1981), and (c) NGC 4565 (from Hama be *et al.* 1980). Solid lines are model profiles, each labelled by its value Of $\log_{10}(\rho_0/\rho_b)$.

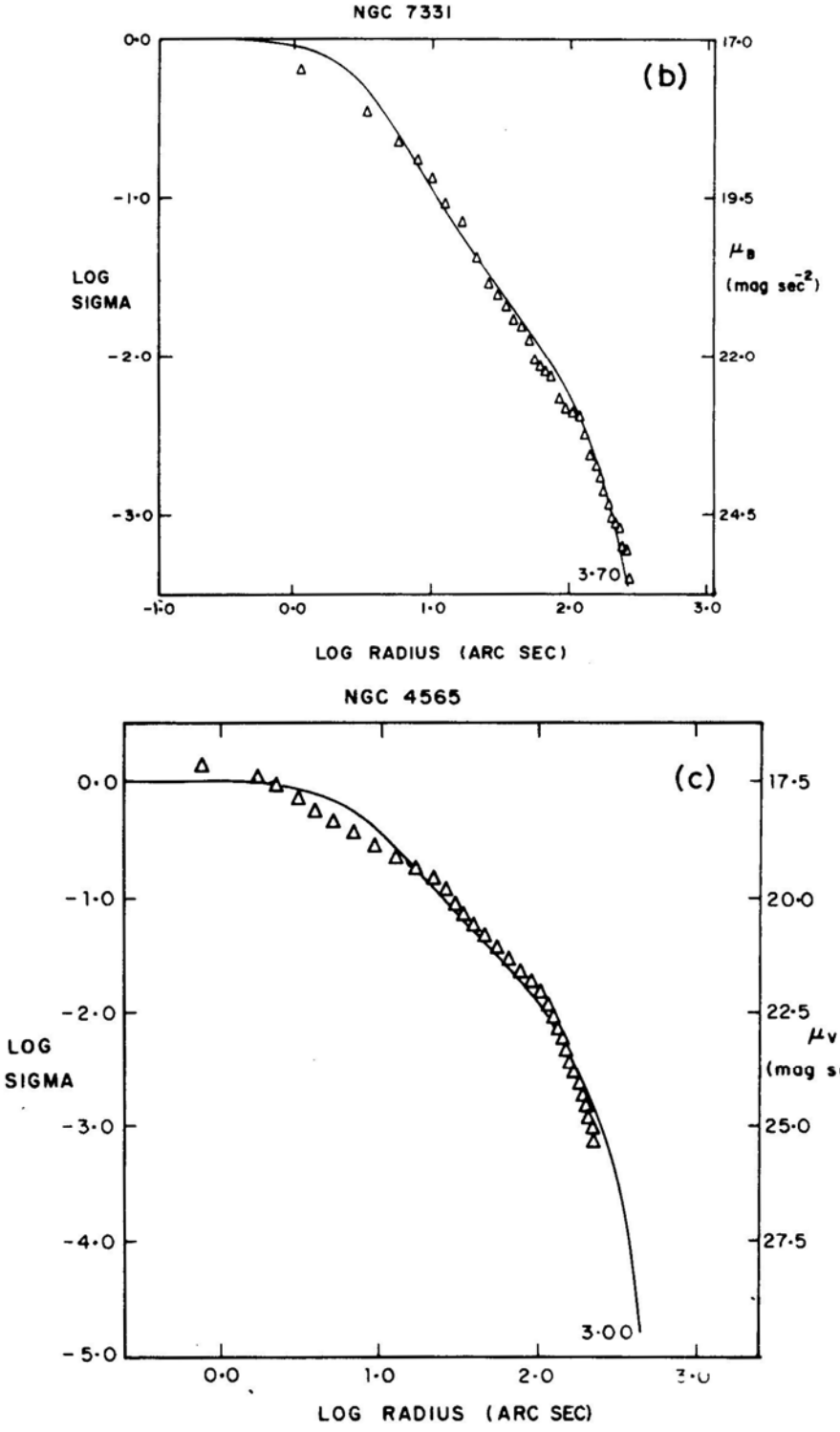

Figure 2. Continued.

discs and $r^{1/4}$ bulges, although it is known that neither functional form has a basis in physics (Boroson 1981; Seiden, Schulman & Elmegreen 1984). We find that our model gives an adequate description of these profiles. Three examples (NGC 2841, 7331 and 4565) of spirals of various sizes and bulge/disc ratios are shown in Fig. 2; more will be given elsewhere (Cowsik & Ghosh 1984). This agreement provides evidence that the distribution of visible matter in spirals is well-approximated by a Maxwellian (see above), and thus provides a physical basis for understanding the shape of luminosity profiles.

3. Discussion

This relatively simple model of a collisionless stellar distribution embedded in a background gas fits so many observations, such as the main features of the rotation curves of spirals (*e.g.* their ubiquitous flatness, gentle increase at large distances and characteristic change in shape with increasing luminosity) and ellipticals, and their luminosity profiles, that it seems worthwhile to consider the nature and composition of the invisible background gas. Quite some time ago, Ostriker & Peebles (1973) guessed at the existence of a massive halo around the Galaxy from the requirement of dynamical stability of the spirals. Many candidates, such as black holes, 'Jupiters', dust, massive neutrinos and exotic particles envisaged in GUTs and SUSYGUTs, have been suggested and their relative merits as the constituents of the 'dark matter' have been assessed (Peebles 1979). For example, the suggestion that 'Jupiters' are the constituent would come into conflict with the distribution of the masses of stars, which shows a flattening even at 0.5 $M_\odot$, so that the initial mass function will have to be bimodal. Further, if the haloes are made of baryonic matter in any form, then the average baryonic matter density in the universe would exceed 10^{-30} g cm^{-3} and the observed abundances of ^{2}D and ^{4}He would be in conflict with the expected abundances from primordial nucleosynthesis. Therefore, it is natural that the explanation for the dark matter has been sought in terms of some weakly interacting non-baryonic relic from the big bang.

The present study of the rotation curves places further constraints on the nature of the dark matter. There are two basic points: First, the density of the background needed to explain the observations is roughly equal to the density of clusters and groups estimated from dynamical considerations (Peebles 1979; Gott & Turner 1977). The large dispersion in velocities of galaxies in clusters (~ 1500 km s^{-1}) naturally fits in with the requirements of the model for the background gas. The minimum mass, m, of the particle which would condense on such a large scale can be estimated from the formula (Cowsik & McClelland 1973).

$$m^8 \gtrsim -\frac{6h^6}{G^3 R_c^3 M_c \alpha^2}. \tag{10}$$

Here, α is the fraction of the total available phase space up to the edge of the cluster that is occupied by the neutrinos. We estimate the filling fraction $\alpha \propto (3v_v/c)^{3/2} \simeq 10^{-3}$ Taking the typical mass of a cluster to be ~ 3×10^{15} $M_\odot$ and a core radius of ~ 0.1 Mpc one finds $m \gtrsim 10$ eV. Second, the systematic progression in the form of the rotation curves of the spirals with their luminosity demands that the density of background be sensibly independent of the size and mass of the spiral galaxy. It would

be difficult to accommodate this requirement in a scenario where more massive particles are involved, be they photinos or gravitinos (Cabbibo, Farrar & Maiani 1981; Pagels & Primack 1981) on the one hand, or black holes or Jupiters on the other, since these would tend to cluster on much smaller scales comparable to that of the underlying galaxies.

In summary, the systematics of the rotation curves of the galaxies can be explained on the basis of a simple model in which a Maxwellian gas is embedded in a background gas with a much larger dispersion in velocities. On the basis of these systematics, it appears that collisionless particles with $m \sim 10$ eV and $M_{J\max} \sim 3 \times 10^{15}\ M_{\odot}$ (Bond, Efstathiou & Silk 1980; Wasserman 1981; Doroshkevich *et al.* 1980; Sato & Takahara 1980), which condense typically on the dimensions of galactic clusters (Cowsik & McClelland 1973; Schramm & Steigman 1980) make up the background gas cloud needed in the model. Among the known particles, only the neutrinos could have the required mass and the weak interactions demanded of the constituents of the dark matter in the universe.

References

Bahcall, J. N., Schmidt, M., Soneira, R. M. 1982, *Astrophys. J.*, **258,** L23.
Binney, J. 1982a, *Mon. Not. R. astr. Soc.*, **200,** 951.
Binney, J. 1982b, *A. Rev. Astr. Astrophys.*, **20,** 399.
Bond, J. R., Efstathiou, G., Silk, J. 1980, *Phys. Rev. Lett.*, **45,** 1980.
Boroson, T. 1981, *Astrophys. J. Suppl.*, **46,** 177.
Bosma, A. 1978, *PhD Thesis,* Groningen Univ.
Bosma, A. 1981, *Astr. J.*, **86,** 1825.
Burstein, D. 1979, *Astrophys. J. Suppl.*, **41,** 435.
Burstein, D., Rubin, V. C., Thonnard, N., Ford W. K. Jr. 1982, *Astrophys. J.*, **253,** 70.
Cabbibo, N., Farrar, G. R., Maiani, L. 1981, *Phys. Lett.*, **105B**, 155.
Chandrasekhar, S. 1939, *An Introduction to the Study of Stellar Structure,* Univ. Chicago Press, p. . 156.
Chandrasekhar, S. 1942, *Principles of Stellar Dynamics,* Dover, pp. 48–85.
Cowsik, R. 1984, *TIFR Preprint,* TIFR-CRSP-84-16.
Cowsik, R., McClelland, J. 1973, *Astrophys. J.*, **180,** 7.
Doroshkevich, A. G. *et al.* 1980, *Ann. NY Acad. Sci.*, **375,** 32.
Einasto, J. 1970, *Teated Tartu Obs.*, **26,** 1.
Emden, R. 1907, *Gaskugeln*, Leipzig, Teubner.
Gott, J. R., Turner, E. L. 1977, *Astrophys. J.*, **213,** 309.
Hamabe, M., Kodaira, K., Okamura, S., Takase, B. 1980, *Publ. astr. Soc. Japan*, **32,** 197.
Jeans, J. H. 1915, *Mon. Not. R. astr. Soc.*, **76,** 71.
Kormendy, J. 1977, *Astrophys. J.*, **217,** 406.
Lynden-Bell, D. 1962, *Mon. Not. R. astr. Soc.*, **124,** 95.
Ostriker, J. P., Caldwell, J. A. R. 1979, in *IAU Symp.* 84: *The Large-Scale Characteristics of the Galaxy,* Ed. W. B. Burton, D. Reidel, Dordrecht, p. 441.
Ostriker, J. P., Peebles, P. J. E. 1973, *Astrophys. J.*, **186,** 467.
Pagels, H., Primack, J. R. 1981, *Phys. Rev. Lett.*, **48,** 223.
Peebles, P. J. E. 1979, in *Physical Cosmology,* Eds R. Balian, J. Audouze & D. N. Schramm, North-Holland, Amsterdam, p. 216.
Rubin, V. C. 1979, in *1 AU Symp.* 84: *The Large-Scale Characteristics of the Galaxy,* Ed. W. B. Burton, D. Reidel, Dordrecht, p. 211.
Rubin, V. C. 1983, in *Kinematics, Dynamics and Structure of the Milky Way,* Ed. W. L. Shuter, Reidel, Dordrecht, p. 379.
Rubin, V. C., Ford, W. K. Jr., Thonnard, N. 1980, *Astrophys. J.*, **238,** 471.

Rubin, V. C., Ford, W. K. Jr., Thonnard, N. 1982, *Astrophys. J.*, **261,** 439.
Sato, H., Takahara, F. 1980, *Prog. Theor. Phys.*, **64,** 2029.
Schramm, D. N., Steigman, G. 1981, *Astrophys. J.*, **243,** 1.
Seiden, P. E., Schulman, L. S., Elmegreen, B. G. 1984, *Astrophys. J.*, **282,** 95.
van der Kruit, P. C. 1979, *Astr. Astrophys. Suppl*., **38,** 15.
van der Kruit, P. C. 1982, *Astr. Astrophys*., **110,** 61.
van der Kruit, P. C., Searle, L. 1981, *Astr. Astrophys.*, **95,** 105.
Wasserman, I. 1981, *Astrophys. J.*, **248,** 1.
Wevers, B. M. H. R. 1984, *PhD Thesis*, Groningen Univ.